

Effect of Magnetic Field on the Rotating Flow in a Similar Czochralski Configuration

Ahmed BOUGHEZALA HAMAD, Said bouabdallah, Salah BOUGHEZALA MOHAMMED

Laboratory of Mechanics, Department of Mechanical Engineering, University of Laghouat BP 37 G, Road of Ghardaia, Laghouat 03000, Algeria.

Laboratory of Mechanics, Department of Mechanical Engineering, University of Laghouat BP 37 G, Road of Ghardaia, Laghouat 03000, Algeria.

Departement of Electrical Engineering , University of Biskra BP 145 RP, 07000

Email: bha20141988@gmail.com

Abstract— We present a numerical study of the rotating flow generated by two rotating disks in co /counter -rotating, inside a fixed cylindrical enclosure similar to the Czochralski configuration (Cz). The enclosure having an aspect ratio $A = H/R_c$ equal to 2, filled with a low Prandtl number fluid, which is submitted to a vertical temperature gradient. The conservation equations governing the studied phenomenon are solved by the method of the finite volume using the FLUENT software 6.3.26. We present the steady state flow; and we make a comparison between the flow generated by the co-/counter-rotating end disks. This study was carried out for different Richardson numbers; $Ri = 0.01, 0.1, 0.5, 1, 2, 3, 5$ and 10 . The effect of orientation of the magnetic field is also taken into account for different values of the Hartmann number ($Ha = 0, 5, 10, 20, 30$ and 50). The obtained results show that the strongest stabilization of the velocity field and heat transfer occurs when the flow generated by co-rotating end disks and the applied of magnetic field in radial direction provided a more stabilization of the convective flow.

Keywords— Rotating Flow, Magnetic Field, axisymmetric cylindrical cavity, finite volume method.

I. INTRODUCTION

The study of a flow shrouded by the rotating bottom of a cylinder aroused a growing interest during the last decades. This interest is dictated by the role played by such a configuration in several fields of the industry such as viscometers, centrifugal machines, the pumping of liquid metals with a high melting point, the production of crystals by the Czochralski drawing process, etc. etc. This configuration has been studied experimentally and numerically for more than thirty years. The first experiments of Vogel [1] showed the suction and pumping of Ekman, induced by these layers on the rotating disk, leads to the formation of a concentrated nucleus along the axis of symmetry. The numerical study of this problem has been made by several researchers such as Hyun [2] Sorensen and Phuoc Loc [3], Lopez and Perry [4] used nonlinear dynamic theory to describe flow kinematics. For experimental studies there is Spohn et al. [5] experimentally studied the balanced flow produced by a rotating bottom in a closed cylindrical container, Escudier [6] used the so-called Laser-induced fluorescence technique to visualize the swirling flow of a fluid (glycerin / water) occupying the entire volume of a cylindrical chamber with a rotating bottom, to control this type of flow in industrial applications. The objective of the present work is to make a numerical study of a rotating flow

generated by the rotation of Co / counter-rotation discs inside a cylindrical chamber filled with liquid silicon. Our numerical simulations were presented, for different values of the Richardson number ($Ri = 0.1, 0.5, 1.0, 3.0, 5.0$ and 10), to see their effects on the value of the Reynolds number (Re).

II. PROBLEM DESCRIPTION AND MATHEMATICAL FORMULATION

The physical system under consideration Fig. 1, is a cylindrical enclosure has a radius R_c and height H , the aspect ratio is fixed ($A = H/R_c = 2$). The enclosure contains a liquid silicon ($Pr = 0.011$), the bottom disk is rotating with a constant angular velocity ($+\Omega$), and maintained at a hot temperature T_h , while the top disk is in co-/counter-rotating and maintained at a cold temperature T_c (we called co-rotating flow when the two end disks rotate in the same direction with Ω , and counter-rotating flow for the opposite directions). The side wall of the cylinder is adiabatic. The system may be subjected to a magnetic field of constant magnitude B , oriented in both axial and radial directions, separately. Adopting the assumptions of [7], and introducing the scales R_c for lengths, ΩR_c for velocities, $\rho(\Omega R_c)^2$ for pressure, $(T_h - T_c)$ for temperature, and $\Omega R_c^2 B$ for electric potential, the dimensionless equations of the system become:

$$\frac{1}{R} \frac{\partial}{\partial R} (R U_r) + \frac{\partial U_z}{\partial Z} = 0 \quad (1)$$

$$\frac{\partial U_r}{\partial \tau} + \left[\frac{1}{R} \frac{\partial}{\partial R} (R U_r^2) + \frac{\partial}{\partial Z} (U_r U_z) + \frac{U_\theta^2}{R} \right] = \quad (2)$$

$$-\frac{\partial P}{\partial R} + \frac{1}{Re} \left[\frac{1}{R} \frac{\partial}{\partial R} \left(R \frac{\partial U_r}{\partial R} \right) + \frac{\partial^2 U_r}{\partial Z^2} - \frac{U_r}{R^2} \right] + N F_{Lr}$$

$$\frac{\partial U_z}{\partial \tau} + \left[\frac{1}{R} \frac{\partial}{\partial R} (R U_r U_z) + \frac{\partial}{\partial Z} (U_z^2) \right] = \quad (3)$$

$$-\frac{\partial P}{\partial Z} + \frac{1}{Re} \left[\frac{1}{R} \frac{\partial}{\partial R} \left(R \frac{\partial U_z}{\partial R} \right) + \frac{\partial^2 U_z}{\partial Z^2} \right] + Ri \cdot \Theta + N F_{Lz}$$

$$\frac{\partial U_\theta}{\partial \tau} + \left[\frac{1}{R} \frac{\partial}{\partial R} (R U_r U_\theta) + \frac{\partial}{\partial Z} (U_z U_\theta) + \frac{U_r U_\theta}{R} \right] = \frac{1}{\text{Re}} \left[\frac{1}{R} \frac{\partial}{\partial R} (R \frac{\partial U_\theta}{\partial R}) + \frac{\partial^2 U_\theta}{\partial Z^2} - \frac{U_\theta}{R^2} \right] + N F_{L\theta} \quad (4)$$

$$\frac{\partial \Theta}{\partial \tau} + \frac{1}{R} \frac{\partial}{\partial R} (R U_r \Theta) + \frac{\partial}{\partial Z} (U_z \Theta) = \frac{1}{\text{Pr}} \left[\frac{1}{R} \frac{\partial}{\partial R} (R \frac{\partial \Theta}{\partial R}) + \frac{\partial^2 \Theta}{\partial Z^2} \right] \quad (5)$$

$$\frac{1}{R} \frac{\partial}{\partial R} (R \frac{\partial \Phi}{\partial R}) + \frac{\partial^2 \Phi}{\partial Z^2} = \left(\frac{U_\theta}{R} + \frac{\partial U_\theta}{\partial R} \right) \quad (6)$$

where $N = Ha^2 / \text{Re}$ and F_{LR} , F_{LZ} and $F_{L\theta}$ are the Lorentz force component in R , Z and θ directions respectively. Thiers expressions were given as following:

- Case of axial magnetic field (B_z):

$$F_{LR} = -U_r \quad F_{LZ} = 0 \quad F_{L\theta} = \frac{\partial \Phi}{\partial Z} - U_\theta \quad (7a)$$

- Case of radial magnetic field (B_r):

$$F_{LR} = 0 \quad F_{LZ} = -U_z \quad F_{L\theta} = -\frac{\partial \Phi}{\partial Z} - U_\theta \quad (7b)$$

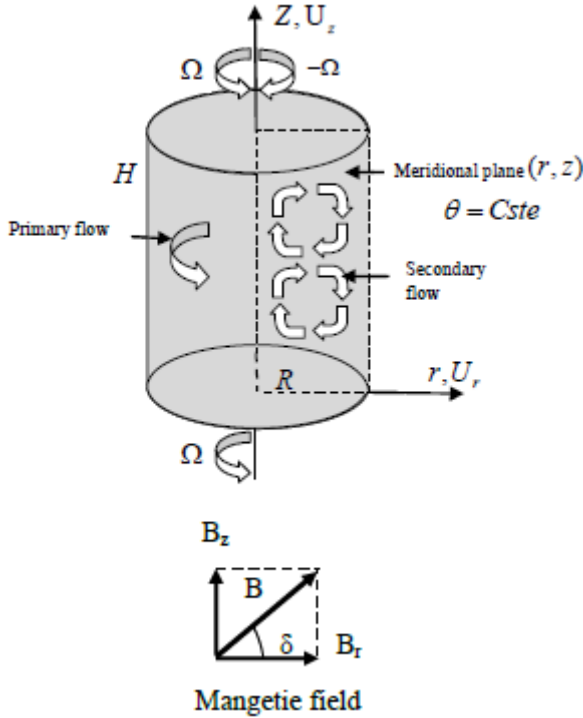


Fig. 1. Sketch of physical problem.

The appear flow parameter in the dimensionless mathematical model are: Reynolds number $\text{Re} = \Omega R^2 / \nu$, Richardson number $\text{Ri} = \text{Gr} / \text{Re}^2$, Grashof number $\text{Gr} = g\beta(\text{Th} - \text{Tc})R^3 / \nu^2$, Prandtl number $\text{Pr} = \nu / \alpha$ and Hartmann number $\text{Ha} = BR \sigma / \rho \nu$ which is indicate the ratio between the electromagnetic force and viscosity force.

The boundary conditions are given as following:

At: $R = 0$ and $0 \leq Z \leq 2$:

$$U_r = U_\theta = \frac{\partial U_z}{\partial R} = 0, \quad \frac{\partial \Theta}{\partial R} = 0, \quad \frac{\partial \Phi}{\partial R} = 0 \quad (8a)$$

At: $R = 1$ and $0 \leq Z \leq 2$:

$$U_r = U_\theta = U_z = 0, \quad \frac{\partial \Theta}{\partial R} = 0, \quad \frac{\partial \Phi}{\partial R} = 0 \quad (8b)$$

At: $Z = 0$ and $0 \leq R \leq 1$:

$$U_r = U_z = 0, \quad U_\theta = R, \quad \Theta = 1, \quad \frac{\partial \Phi}{\partial R} = 0 \quad (8c)$$

At: $Z = 2$ and $0 \leq R \leq 1$:

$$U_r = U_z = 0, \quad U_\theta = R, \quad \Theta = 0, \quad \frac{\partial \Phi}{\partial R} = 0 \quad (8d)$$

III. VALIDATION AND COMPARISON OF RESULTS

In order to give more confidence to the results of our numerical simulations, a comparison was made with the experimental investigation obtained by Michelson [8], who used the LDA (Laser Doppler Anemometry) technique to determine the axial distribution of the azimuthal velocity at $r = 0.60$ in a cylindrical cavity, whose upper disk is in rotation, and that for $\text{Re} = 1800$ and $\gamma = 1$ (Fig.2). It is easy to see that the calculated values are in excellent agreement with the measurements in the whole flow field.

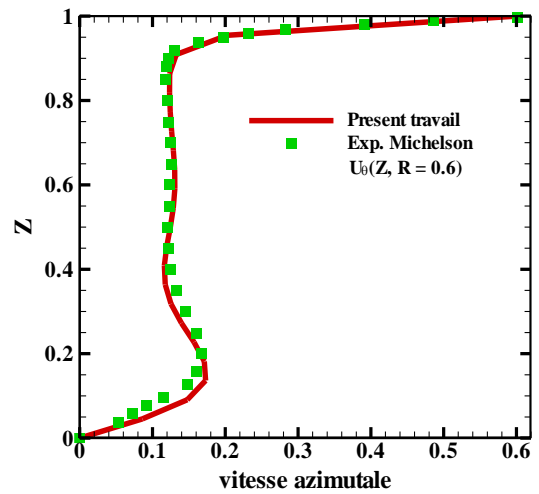


Fig. 2. Profils de la composante de vitesse azimuthale à $R = 0.6$

IV. RESULTS AND DISCUSSION

A. case of Natural convection:

To study the effect of the intensity of the magnetic field on natural convection, we have set the Grashof number to $Gr = 10^6$ and we vary the Hartman number so that Ha takes the following values: $Ha = 0, 5, 10, 20, 30$ and 50 . In the figure (Fig.3) we presented the axial velocity profiles U_z .

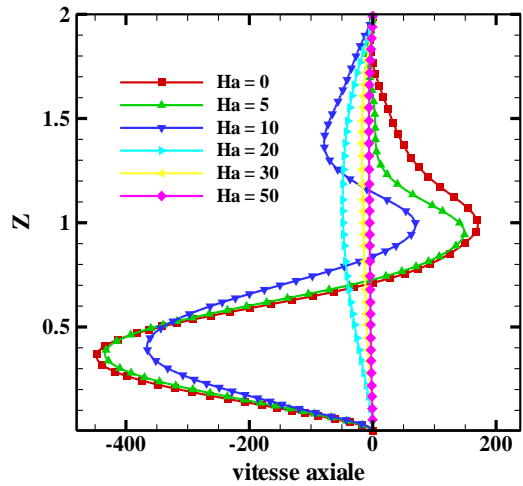
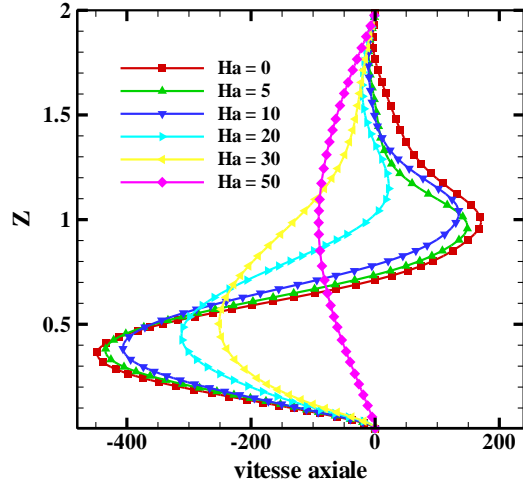


Fig. 3. Axial velocity component profiles at $R = 0.5$, for $Gr = 10^6$ and, for different Hartman number values applied to axial and radial direction respectively.

B. case of Mixed convection:

To study the effect of the magnetic field intensity and their orientation in both axial and radial directions on mixed convection, we have set the Richardson number to $Ri = 10$ and we vary the number of Hartman (in both directions: axial and radial separately) so that Ha takes the following values: $Ha = 0, 5, 10, 20, 30$ and 50 . In Figures 4, (1.2), 6 and 7 we presented the current lines, isotherms and contours of the azimuthal velocity component.

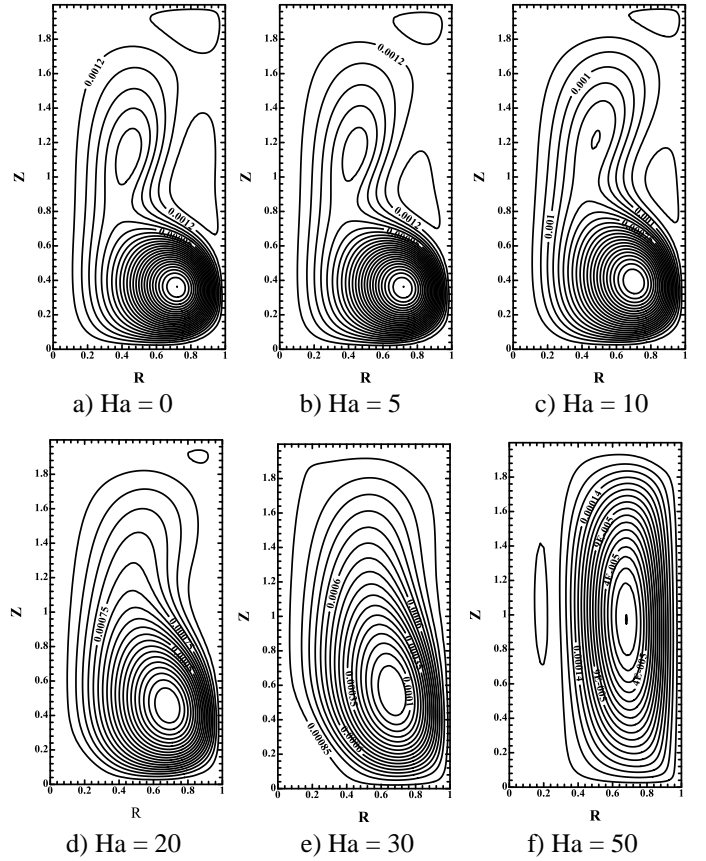


Fig. 4. Current lines for different Hartman number values applied to the axial direction.

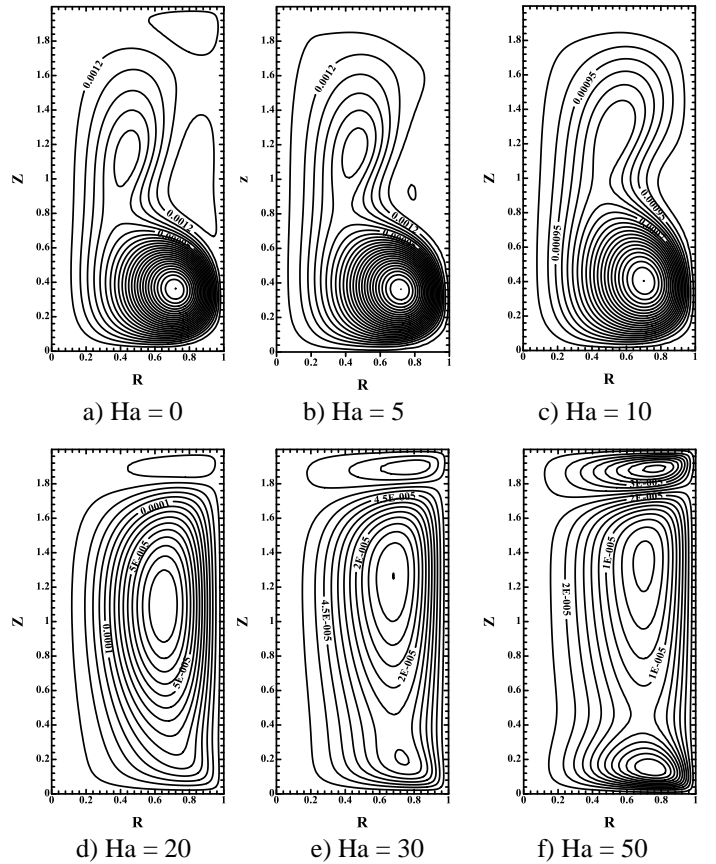
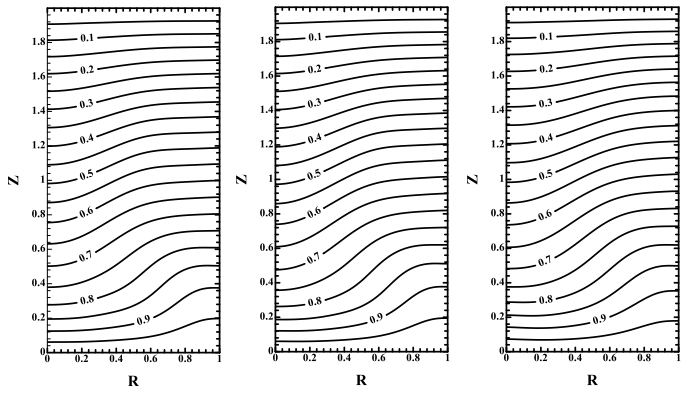


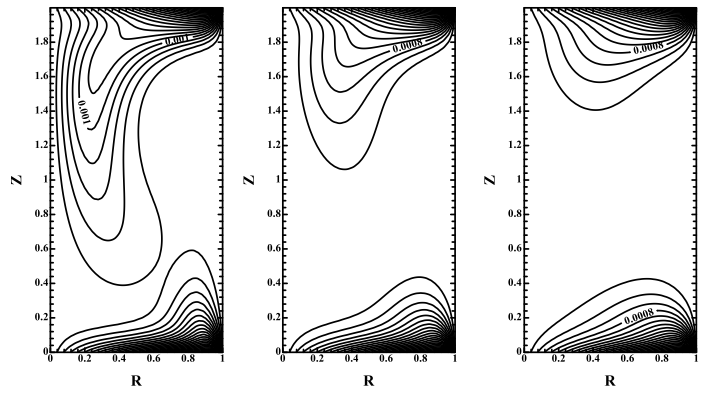
Fig. 5. Current lines for different Hartman number values applied to the radial direction.



a) $Ha = 0$

b) $Ha = 5$

c) $Ha = 10$

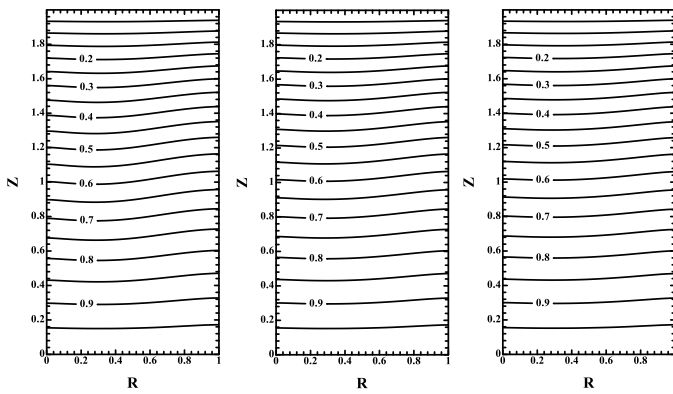


d) $Ha = 20$

e) $Ha = 30$

f) $Ha = 50$

FIG. 7. Contours of the azimuthal velocity component, for different Hartman number values applied to the radial direction.

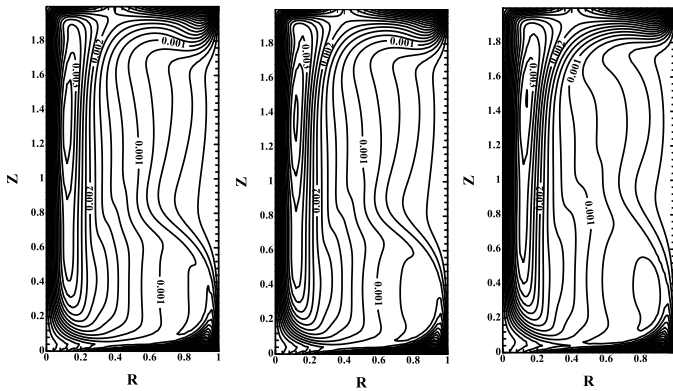


d) $Ha = 20$

e) $Ha = 30$

f) $Ha = 50$

Fig. 6. Isothermal lines for different Hartman number values applied to the radial direction.



a) $Ha = 0$

b) $Ha = 5$

c) $Ha = 10$

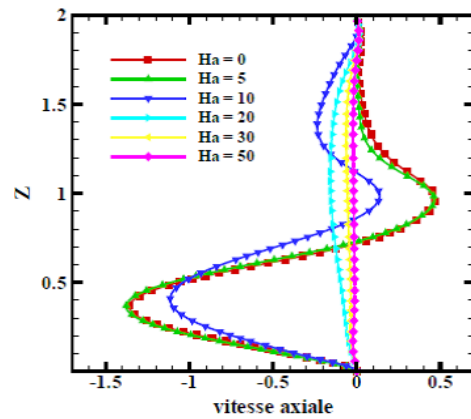
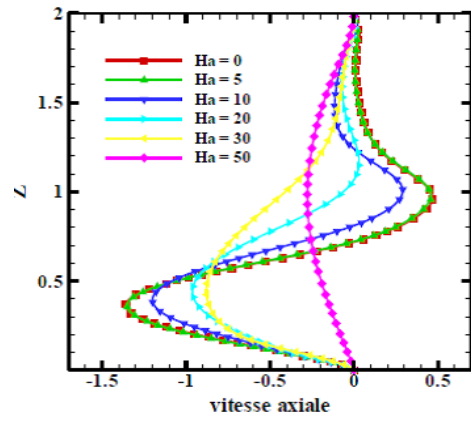


Fig. 8. Axial velocity component profiles at $R = 0.5$, for $Gr = 10^6$ and, for different applied Hartman number values applied to axial and radial direction respectively.

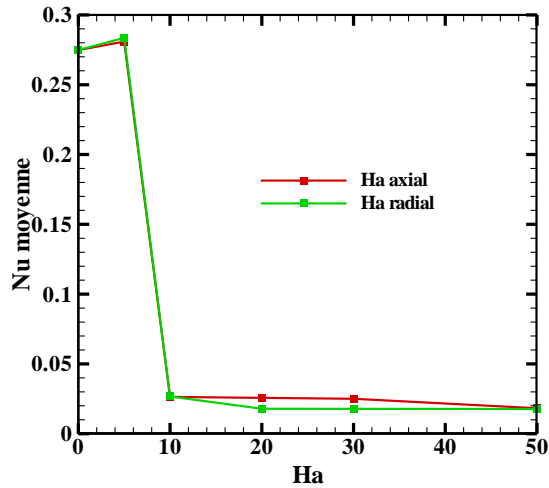


Fig. 9. Average number of Nusselt depending on the number of Hartman applied to the axial and radial direction.

The variation in the number average Nusselt number as a function of Hartman (Ha) applied in the axial and radial direction is shown in Fig.9. We notice that the number of Nusselt decreases with the increase of Ha ideally in the case of the application of the magnetic field to the radial direction

CONCLUSION

A numerical study of the rotating flow generated by two rotating disks in co-/counter-rotating direction, inside a cylindrical enclosure similar to Cz configuration was carried out. Comparisons with published work on specific cases are performed and found to be in good agreement. From the obtained results, the following conclusions are drawn:

- The comparison between the flow generated by the co-rotating and counter-rotating disks shows that the strongest stabilization of the velocity field and heat transfer occurs when the flow generated by co-rotating end disks.
- The increase of Ri affects straightly on the structure of the flow in both cases co-/counter-rotation, wherever the velocity field and heat transfer rate are destabilized.
- In the presence of the magnetic field, the flow is more regular. An increase in the intensity of the magnetic field causes a change in the magnitude and flow structure, where is stabilize the velocity field and heat transfer rate.
- A more reduction of the velocity field and heat transfer rate is important when the radial magnetic field is applied (B_r).

REFERENCES

- [1] Vogel, H. U., Experimentelle Ergebnisse über die laminäre Strömung in einem zylindrische Gehäuse mit darin rotierender Scheibe, *Phys. Fluids* 6, 2702 -1968 (1968).
- [2] Hyun J. M., Flow in an open tank with a free surface driven by the spinning bottom, *J. Fluid Eng.* 107,495 (1985).
- [3] Sorensen J. N., and Loc, T. P., High-order axisymmetric Navier-Stokes code: Description and evaluation of boundary conditions, *Int. J. Numer. Meth. Fluids* .9, 1517-1537 (1989).
- [4] Lopez J. M., Axisymmetric vortex breakdown part 1. Confined swirling flow, *J. Fluid Mech.* 221, 533-552 (1990).
- [5] Spohn, A., Mory, M. and Hopfinger, E. J. Observations of vortex breakdown in an open cylindrical container with a rotating bottom. *Experiments in Fluids*. 14, 70-77 (1993).
- [6] Escudier, M., "Observations of the flow produced in a cylindrical container by a rotating endwall", *Experiments in fluids*, Vol. 2, No. 4, (1984), 189 -196.
- [7] Mahfoud, B. and Bessaih, R., "Oscillatory swirling flows in a cylindrical enclosure with co-/counter-rotating end disks submitted to a vertical temperature gradient", *Fluid Dynamics & Materials Processing*, Vol. 8, No. 1, (2012), 1-26.
- [8] Michelson, J.A, "Modeling of laminar incompressible rotating fluid flows", AFM 86-05, Ph. D. Dissertation. Dept. of Fluid Mechanics, Tech. Univ. of Denmark (1986).